



Advanced Sustainable Foundry

19-21 May 2014 • Palacio Euskalduna, BILBAO

19-21 May 2014 • Palacio Euskalduna, BILBAO



Effect of microalloying element addition on the microstructure, mechanical and corrosion behaviour of A356 secondary alloy with 0.30wt% Fe

(A. Niklas)

IK4-AZTERLAN, Engineering, R&D and Metallurgical Processes, Durango, Spain

(R. González-Martínez)

IK4-AZTERLAN, Engineering, R&D and Metallurgical Processes, Durango, Spain

(F. Sáenz de Tejada)

Befesa Aluminio S.L. Erandio, Spain

(A. Conde)

Centro Nacional de Investigaciones Metalúrgicas, CENIM (CSIC), Spain

(M. A. Arenas)

Centro Nacional de Investigaciones Metalúrgicas, CENIM (CSIC), Spain

(J. J. de Damborenea)

Centro Nacional de Investigaciones Metalúrgicas, CENIM (CSIC), Spain

(R. Suárez)

IK4-AZTERLAN, Engineering, R&D and Metallurgical Processes, Durango, Spain
Veigalan Estudio 2010 SLU, Durango, Spain

(S. Méndez)

IK4-AZTERLAN, Engineering, R&D and Metallurgical Processes, Durango, Spain

Copyright 2014 World Foundry Organization

ABSTRACT

This work investigated how trace additions of Mn, Cr and V affect the morphologies of harmful β -AlFe5Si intermetallics, mechanical properties and corrosion behavior of A356 secondary alloy with an iron content of 0.30wt%. The needle shaped β -intermetallics are replaced by a Chinese script α - compound when Mn, Cr and V are added. The mechanical properties of A356 secondary alloys were improved by the modification of the β -intermetallics into α -iron compounds. The corrosion behavior of the modified secondary alloy was similar to both, the A356 primary and the unmodified secondary alloys. Thus, small additions of Mn, Cr and V improve the mechanical properties without negatively affecting the corrosion resistance of A356 secondary alloy.

Keywords: A356 alloy, corrosion, β -iron phases, α -iron phases, secondary alloy, mechanical properties.

1. INTRODUCTION

Primary aluminium alloys are widely used in the manufacturing of safety parts for the automotive industry due to their good mechanical properties. In contrast secondary aluminium alloys are rich in impurities, in particular in iron, resulting in worse mechanical properties when compared to the corresponding primary alloys¹. This is because of the presence of harmful β -iron compounds which tend to initiate cracks and provide easy pathways for crack propagation²⁻³. Therefore, these alloys are nowadays not used in the manufacturing of safety parts with high mechanical requirements. However, the use of recycled alloys has increased considerably because



of potential energy savings, and generates less CO₂ emission compared to primary aluminium production⁴. The addition of trace elements like Mn, Be, V, Cr, and Co could improve the quality of secondary alloys with high iron content.⁵⁻¹⁰ because they prevent the formation of β -Al₅FeSi phases by changing the morphology of the β -Al₅FeSi phase into a less harmful one (Chinese script or globular). However, by introducing additional alloying elements the overall amount of intermetallic compounds increases¹¹.

The present work investigates the effect of additions of Mn, Cr and V on the morphology of the intermetallic iron compounds, mechanical properties and corrosion resistance of A356 secondary alloy and the corresponding A356 primary alloy.

2. DESIGN OF EXPERIMENTS

2.1. TEST MATERIALS

Three alloys were prepared by melting commercial A356 alloys: a) primary alloy A356, b) secondary alloy (A356 with 0.30 wt% Fe) and c) secondary alloy modified with Mn, Cr and V additions in form of master alloys. The amount of additions has been optimized in a previous investigation¹¹. The chemical compositions of these alloys were analyzed by spark emission spectrometer (Spectrolab) and are presented in Table 1. For each experiment, 40 kg of each alloy were melted in an electric furnace with a capacity of 60 kg. The alloys were modified using AlSr10 master alloy and refined using AlTi5B1 master alloy. The melt was degassed with nitrogen gas for 20 min using a graphite lance. Then the melts were poured into a sand moulds at a temperature between 720 °C and 740 °C and rectangular test samples with dimensions of 190x90x12mm were obtained.

2.2. HEAT TREATMENT, MICROSTRUCTURE CHARACTERIZATION AND TENSILE TESTING

The alloys were heat treated to the T6 condition consisting of a solution heat treatment at 540°C for 8h, followed by water quenching to ambient temperature, and subsequent artificial aging at 155 °C for 8h. The characteristics and chemical composition of the intermetallic iron compounds were examined using scanning electron microscopy (SEM) equipped with an energy dispersive X-ray spectrometer (EDS). For the quantification of length and area fraction of both β and α iron compounds, twenty images were obtained at a magnification of 2000X. The plate length for the

β -compounds and the longest dimension for the α -compounds were measured, respectively. The area fraction and length of each compound was estimated using a LAS V4.2 image analyzer. Tensile test specimens were machined and tested according to UNE-EN ISO 6892-1:2010. For each alloy three test specimens were tested

2.3. SALT SPRAY TEST

Salt spray testing was conducted in accordance with ASTM B117. Test samples in the shot blasted state with dimensions 190x90x12mm were exposed for 336h in a salt fog chamber WEISS SC/KWT 10000 (pulverised solution of 5% NaCl, 35°C and Hr >95%). At the end of the test, samples were cleaned according to ISO 8407:2009 and visual inspected.

2.4. ELECTROCHEMICAL MEASUREMENTS

Electrochemical tests were performed in a 0.03 M NaCl solution by means of a Gamry Reference 600 potentiostat using a conventional three-electrode cell: the working electrode is the specimen under study; saturated Ag/AgCl was used as the reference electrode; and a spring platinum wire was used as the counter-electrode. In all cases, the tested area was approximately 1.20 cm². The tests were performed at ambient temperature and in triplicate. The potential was scanned at a rate of 0.167mV/s from an initial potential of -0.3 V, with respect to the open circuit potential, to a potential at which the specimen reached a current density of 0.25mA/cm².

3. RESULTS AND DISCUSSION

3.1. EFFECT OF ALLOYING ELEMENTS ON THE MICROSTRUCTURE

The microstructure of the primary A356, secondary A356 and modified secondary alloy with T6 heat treatment are shown in the Figure 1.

The microstructure of the A356 primary alloys (Figures 1a-b) is typical of hypoeutectic aluminium-silicon alloy consisting of α -aluminium, eutectic silicon and platelet shaped β -Al₅FeSi and Chinese script π -Al₈Si₆Mg₃Fe iron compounds. The secondary alloy with high Fe content (Figures 1c-d) reveals the formation of large β needles. With increasing the Fe content to this alloy, up to 0.30 wt%, the number and length of β needles was increased. In the modified secondary alloy (Figures 1e-f) it can be observed that the harmful β -phases are almost completely

71ST
BILBAO
2014



WORLD
FOUNDRY
CONGRESS



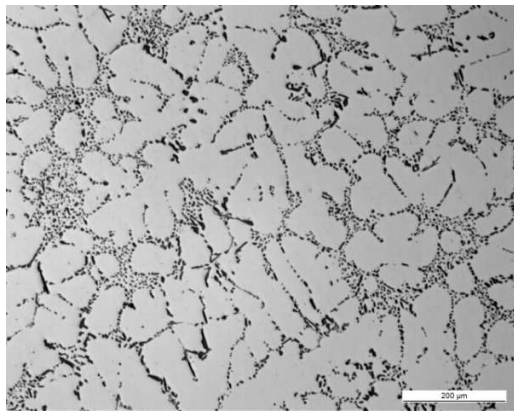
Advanced Sustainable Foundry

19-21 May 2014 • Palacio Euskalduna, BILBAO

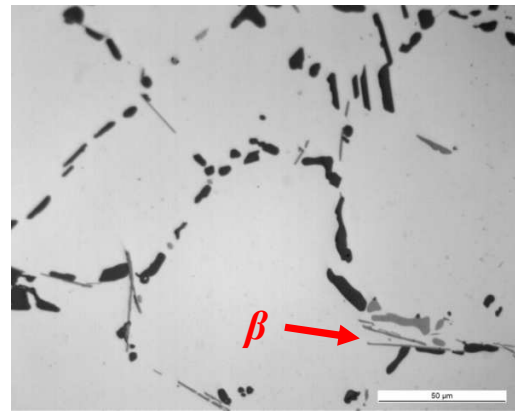
replaced by α - iron compounds of the $Al_{15}(FeMnCrV)_3Si_2$
type with a less harmful chinese script morphology.

Table 1. Chemical composition (wt. %)

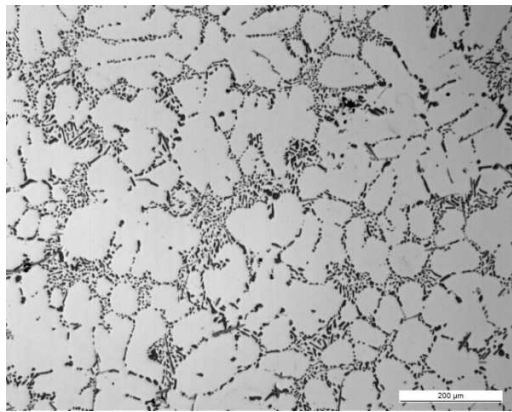
Alloy	Si	Fe	Cu	Zn	Mg	Mn	Cr	Ti	V	Sr
Primary A356	6.74	0.19	<0.01	<0.01	0.50	0.01	<0.01	0.16	0.006	0.014
Secondary A356 alloy	7.25	0.30	0.05	0.05	0.50	0.05	<0.01	0.17	0.009	0.015
Modified secondary alloy	6.72	0.30	0.04	0.05	0.46	0.11	0.12	0.16	0.040	0.015



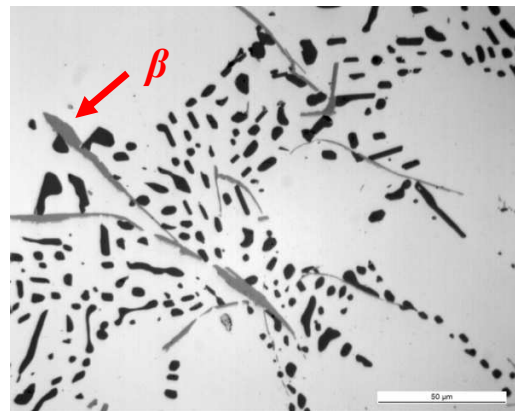
(a)-200x



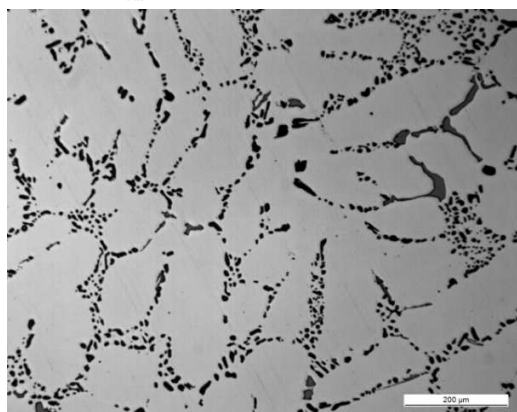
(b)-500x



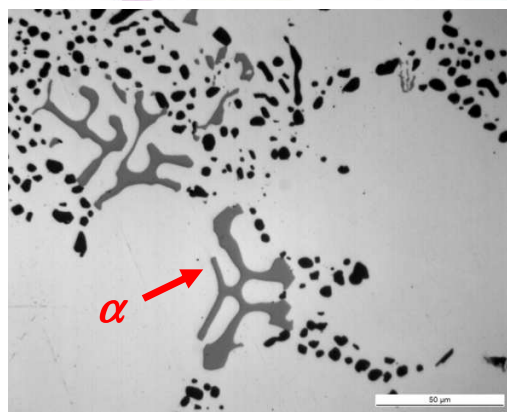
(c)-200x



(d)-500x



(e)-200x



(f)-500x

Fig. 1. Optical microstructure of the a-b)primary A356, c-d)secondary alloy and e-f)modified secondary alloys.

In table 2 the measured characteristic of α and β -iron compounds are summarised. The length and area fraction occupied by the β -compounds increases with increasing iron content and decrease with increasing the content of modifying elements.

It can be observed that when microadditions of Cr, Mn and V are made, the β -iron compounds are transformed almost completely into α -iron compounds. The large α -compounds have a size between 70–340 μm .

Table 2. Characteristics of intermetallic iron compound

Alloy	Characteristics of iron compounds					
	Average Length		Maximum Length		Area Fraction	
	β (μm)	α (μm)	β_{max} (μm)	α_{max} (μm)	A_{β} (μm)	A_{α} (μm)
Primary A356	37	-	87	-	0.15	-
Secondary alloy	70	-	155	-	0.85	-
Modified secondary alloy	55	77	69	340	0.03	1.3

A semi-quantitative EDX-analysis of the chemical composition has been conducted on 10 representative α - and β -iron compounds in each alloy. The measured average compositions are summarized in Table 3. Additionally, the morphology of some analyzed α - and β -compounds and the corresponding chemical composition are presented in Figure. 1. It can be observed that the β -compounds of the secondary base alloy contain small amounts of Mn. This element was already present in the recycled base alloy.

Table 3. Chemical composition average of α and β compounds

Alloy	Compound	Al	Si	Fe	Mn	Cr	V
Primary A356	β	59.4	16.3	24.3	-	-	-
Secondary alloy	β	61.9	18.7	17.9	1.3	-	-
Modified secondary alloy	α	59.1	11.8	14.8	5.5	7.9	0.9

3.2. EFFECT OF ALLOYING ELEMENTS ON THE CORROSION RESISTANCE

The figure 2 shows the surface of the test samples of the primary A356 (Figure 2a), secondary A 356 alloy (Figure 2b) and modified secondary alloys (Figure 2c) after the 336 hours exposure in the salt spray chamber. The appearance of specimen after test shows no significant difference on the corroded surface.



a) Primary A356 alloy



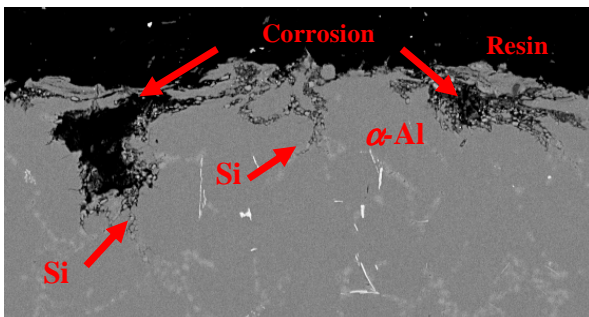
b) Secondary A356 alloy



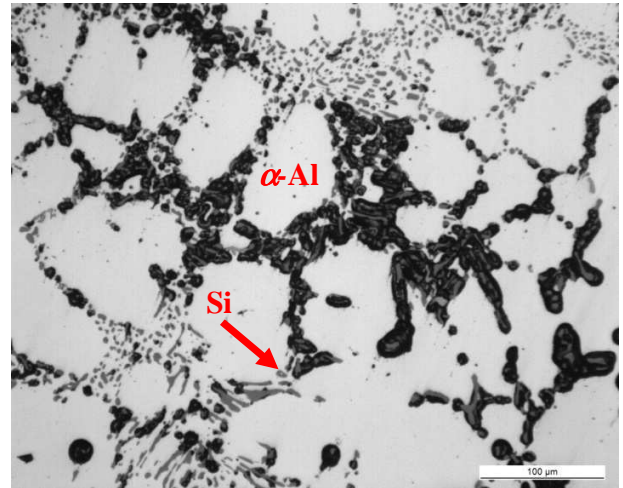
c) Modified A356 secondary alloy

Fig. 2. Salt spray test of a) primary A356, b) secondary A356 alloy, c) modified A356 secondary alloy

Figure 3 shows the scanning electron microscope and optical microscope micrographs of the cross-section and the surface of the corroded modified secondary alloy. It can be seen that the corrosion progress preferentially through the eutectic areas and not at the intermetallic iron compounds. These results are consistent with those described by other authors¹²⁻¹⁴.



a) Cross-section of the corroded surface.



b) Corroded surface.

Fig. 3. Corrosion of modified A356 secondary alloy

The corrosion potential measured along 168h, remained practically constant since the beginning of the experiment and it is practically the same for all the samples -800mV (vsAg/AgCl), figure 4.

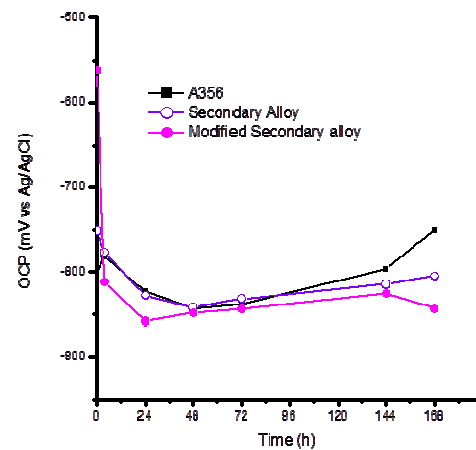


Figure 4 . Variation of corrosion potential along time.

In order to study the corrosion kinetics, potentiodynamic polarization curves were performed on the three alloys (primary A356, secondary and modified secondary alloy). Figure 5 shows the polarization curve of primary A356, secondary and modified secondary alloys in 0.03 M NaCl solution. As it can be seen, the curves for the different samples pictured a similar behavior in their shapes in spite of the variation in their composition and microstructure. The anodic curve seems to present a



pseudo-passive behavior characterized by a slow increase of the currents density with the potential. All the specimens were found to possess a near-equal pitting potential (Epit), with an average value of about -590mV vs Ag/AgCl. The corrosion rate could be estimated close to $5 \times 10^{-7} \text{ Acm}^{-2}$. Anyway, this kind of behavior reveals a material under activation control. Although aluminum cast alloys tending to form a compact layer of hydrated aluminum oxide on its surface, the presence of Cl^- ions interact with the film promoting its dissolution.

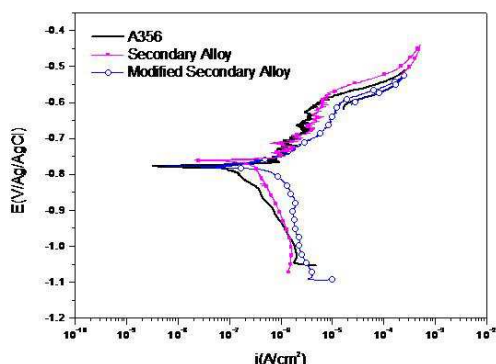


Fig. 5 Polarization curves of the secondary alloys

The cathodic curve for oxygen reduction is quite different than the anodic one. For both secondary alloys, electrode potentials more negative than the E_{corr} , the current density is almost independent of the electrode potential. This is classical behavior of materials under concentration control and is a characteristic curve for the diffusion-limited reduction of oxygen¹⁴. Nevertheless, we should note that compositional modification of the alloy does not have a detrimental effect on the corrosion resistance properties of the unmodified alloy.

3.3. Effect of microalloying elements on mechanical properties

The tensile properties obtained for each alloy are presented in Table 4. It can be seen that the mechanical properties comparable to the ones of the corresponding primary can be achieved by appropriate additions of alloying elements. For comparison of the mechanical properties of the different alloys the quality index Q was also determined. The quality index, $Q = \text{UTS} + K \cdot \log E$, relates the tensile strength, UTS, and the elongation, E , by the coefficient K ¹⁵⁻¹⁸. The parameter K is an empiric coefficient and was found to be 150 MPa for AlSi7Mg alloy. Both parameters Q and K are independent of the heat treatment for this alloy.

As expected, the lowest Q value of 370 MPa was obtained for the unmodified secondary alloy with the highest β -compound area fraction of 0.85 %. In contrast a high Q value of 413 MPa, was achieved for the modified secondary alloy. This value is very similar to the Q value of the primary alloy.

Table 4. Mechanical properties of the alloys

Alloys	UTS (MPa)	YS (MPa)	E (%)	Q (MPa)
Primary A356	283	208	8.0	419
Secondary alloy	262	195	5.3	370
Modified secondary alloy	274	200	8.5	413

CONCLUSIONS

The effect of small microadditions of Cr, Mn and V on the morphology of iron-compounds, mechanical properties and corrosion behavior in A356 secondary alloy has been investigated and compared to the corresponding A356 primary alloy. The following conclusions have been drawn:

- The quality index, $Q = \text{UTS} + K \cdot \log E$, was found to decrease strongly by the presence of β -Al₅FeSi compounds.
- Additions of Mn, Cr and V are very effective to substitute the harmful β -Al₅FeSi compounds by Chinese script α -iron compounds.
- Mechanical properties comparable to the ones of the corresponding primary alloy have been achieved by appropriate additions of alloying elements.
- No significant differences in the corrosion behavior have been observed in the salt spray and electrochemical test.
- This was confirmed by the metallographic analysis which revealed that corrosion occurred preferentially through the eutectic regions and not at the intermetallic iron compounds.
- Thus, A356 secondary alloys with a Fe content of 0.3 wt.% Fe and modified with small Mn, Cr and V additions could be used for applications with high quality requirements without affecting negatively the mechanical properties or the corrosion behavior in a saline environment.
- Corrosion behavior remains unchanged in spite of the compositional modifications.



Advanced Sustainable Foundry

19-21 May 2014 • Palacio Euskalduna, BILBAO



ACKNOWLEDGMENT

Financial support from the Basque Government (Project: ProFUTURE: Factory of the future, Etor tek 2010) is gratefully appreciated

1. Gruzleski, J., Closset, B. M., "The treatment of liquid aluminium-silicon alloys", American Foundry's Society, IL (1990).
2. Crepeau, P. N., Effect of Iron in Al-Si Casting Alloys: A critical Review, AFS Transaction pp. 361-365 (1995).
3. Ma, Z., A.M. Samuel, F.H. Samuel, H. W. Doty, S. Valtierra, A study of tensile properties in Al-Si-Cu and Al-Si-Mg alloys: Effect of β -iron intermetallic and porosity. *Materials Science and Engineering A* 490, pp. 36-51 (2008).
4. Lenka. H., Tillanová Eva, Chalupová María, Piatkowski Joroslav, Optical and Scanning Electron Microscope Studies of Recycled (secondary) Al-Si Cast Alloys, *Solid State Phenomena Vols 203-204* pp. 266-271 (2013).
5. Kim, H.Y., S.W. Han, H.M. Lee, The influence of Mn and Cr on the tensile properties of A356-0.20Fe alloy, *Materials. Letters. Vol. 60*, pp. 1880-1883. (2006).
6. Sreeja S.S., Kumari, R.M. Pillai, K. Nogita, A.K. Dahle, B.C. Pai, Influence of calcium on the microstructure and properties of an Al-7Si-0.3Mg-xFe alloy, *Metallurgical. Materials Transactions. A, Vol. 37A*, pp. 2581-2587, (2006).
7. Murali, S., K.S. Raman, K.S.S. Murthy, Effect of trace additions (Be, Cr, Mn and Co) on the mechanical properties and fracture toughness of Fe-containing AlSi7Mg0.3 Alloy, *Casting Metallurgica. Vol. 6*, pp.189-198, (1994).
8. Samuel, A.M., F.H. Samuel, H.W. Doty, Observations on the formation of β -Al₅FeSi in 319 type Al-Si alloys, *Journal of Materials. Science, Vol. 31*, 1996, pp. 5529-5539, (1996).
9. Lu, L., A.K. Dahle, Iron-rich intermetallic phases and their role in casting defect formation in hypoeutectic Al-Si alloys, *Metallurgical Materials. Transaction. A, Vol. 36A*, 2005, pp. 819-835, (2005).
10. Gustafsson, G., T.Thorvaldsosson, G.L. Dunlop, The influence of Fe and Cr on the microstructure of cast Al-Si alloys, *Metallurgical Transactions A, Vol. 17A*, 1986, pp. 45-52, (1986).
11. de la Fuente E., I. Alfaro, A. Niklas, I. Anza, A.I. Fernández-Calvo. 8th Aluminium Two Thousand Congress. "Improved microstructure and mechanical properties of a recycled AlSi7Mg 0.3 alloy with 0.3 WT% FE by small additions of Mn, Cr and V". 14-18 May, Milano, Italy (2013).
12. Ahlatchi, H., Production and corrosion behaviours of the Al-12Si-XMg alloys containing in situ Mg₂Si particles, *Journal of Alloys and Compounds* 503 pp. 122- 126 (2010).
13. Szklarska-Smialowska, Z., *Corrosion Science Vol. 41, Issue 9*, pp. 1743-1767 (1999).
14. Scully, J. R., D. E. Peebles, A.D. Romig, D.R. Frear, C. R. Hills, Metallurgical factors influencing the corrosion of aluminium, Al-Cu, and Al-Si alloy thin films in dilute hydrofluoric solution, *Metallurgical Transaction A, Vol. 23*, pp 2641-2655 (1992).
15. McCafferty E., "Introduction to Corrosion Science". Chapter 8. Springer Science+Business Media, LLC. New York, (2010)
16. Drouzy. M., S. Jacob, M. Richard, Le diagramme charge de rupture – allongement des alliages d'aluminium. L'indice de qualité application aux A-S7G, *Fonderie 355*, April (1976).
17. Caceres, C.H., A rationale for the quality index of Al-Si-Mg casting alloys », *International Journal of Casting Metals Research.*, , 10, pp. 293-299. (1998)
18. Jacob, S., Quality Index in Prediction of Properties of Aluminium Castings – A Review , *AFS Transactions* 99-209, pp. 811 – 819 (2000).